Vibrational Analysis of Amino Acids and Short Peptides in Hydrated Media. II. Role of KLLL Repeats To Induce Helical Conformations in Minimalist LK-Peptides

ARTICLE *in* THE JOURNAL OF PHYSICAL CHEMISTRY B · DECEMBER 2007

Impact Factor: 3.3 · DOI: 10.1021/jp074264k · Source: PubMed

5 AUTHORS, INCLUDING:

Belén Hernández
Université Paris 13 Nord
39 PUBLICATIONS **375** CITATIONS
SEE PROFILE

Mahmoud Ghomi
Université Paris 13 Nord
112 PUBLICATIONS **1,774** CITATIONS
SEE PROFILE

Vibrational Analysis of Amino Acids and Short Peptides in Hydrated Media. II. Role of KLLL Repeats To Induce Helical Conformations in Minimalist LK-Peptides

Guy Guiffo-Soh,[†] Belén Hernández,[†] Yves-Marie Coïc,[‡] Fatima-Zohra Boukhalfa-Heniche,[†,§] and Mahmoud Ghomi*[,†]

UMR CNRS 7033, BioMoCeTi, UFR SMBH, Université Paris 13, 74 rue Marcel Cachin, 93017 Bobigny cedex, France, Université Pierre et Marie Curie, Case 138, 4 Place Jussieu, 75252 Paris cedex 05, France, and Unité de Chimie Organique, Institut Pasteur, 28 rue du Docteur Roux, 75724 Paris cedex 15, France

Received: June 1, 2007; In Final Form: August 17, 2007

Aqueous solution secondary structures of minimalist LK-peptides, with the generic sequence defined as KLL-(*KLLL*)$_n$KLLK, have been analyzed by means of circular dichroism (CD) and Raman scattering techniques. Our discussion in the present paper is mainly focused on four synthetic peptides (from 5 to 19 amino acids), *KLLL*K, KLL*KLLL*KLLK, KLL*KLLLKLLL*KLLK, and KLL*KLLLKLLLKLLL*KLLK, corresponding to the repeat unit, and to the peptide chains with the values of $n = 1-3$, respectively. CD and Raman spectra were analyzed in order to study both structural features of the peptide chains and their capability to form aggregates. On the basis of the obtained results it was concluded that the conformational flexibility of the shortest peptides (5-mer and 11-mer) is high enough to adopt random, β-type, and helical chains in aqueous solution. However, the 11-mer shows a clear tendency to form β-strands in phosphate buffer. The conformational equilibrium can be completely shifted to β-type structures upon increasing ionic strength, i.e., in PBS and tris buffers. This equilibrium can also be shifted toward helical chains in the presence of methanol. Finally, the longest peptides (15-mer and 19-mer) are shown to form α-helical chains with an amphipathic character in aqueous solution. The possibility of bundle formation between helical chains is discussed over the temperature-dependent H−D exchange on labile hydrogens and particularly by considering the particular behavior of an intense Raman mode at 1127 cm^{-1} originating from the leucine residue side chain. The conformational dependence of this mode observed upon selective deuteration has never been documented up to now.

I. Introduction

The interaction of peptides (and proteins) with cell membranes and model membranes, is known to be monitored by their secondary structure. Especially, those minimalist peptides[1] with amphipathic α-helices have shown optimal interaction with plasma membrane.[1−6] Moreover, it was generally thought that the biological activity of these amphipathic α-helix peptides results from their self-aggregation through membrane bilayers, leading to the formation of channels in which the peptide lipophilic faces interact with phospholipid chains while their hydrophilic residues are oriented inside channels.[1,7−9] Studies at the molecular level by means of spectroscopic techniques (i.e., circular dichroism, FT-IR, Raman scattering, and fluorescence) have provided information on specific structure−function relationships of peptide−model membrane interactions.[8] Leucine−lysine (LK) minimalist peptides are known for their efficiency as antimicrobial[5−9] and nucleic acid delivery agents.[10−12] We emphasize here the first report on antimicrobial LK-peptides by means of the reverse phase high-performance liquid chromatography (RP-HPLC) technique which permitted the correlation between retention times and secondary structures at the water/lipids interface.[7] One of the mentioned peptides was found to adopt an amphipathic α-helix conformation upon interacting with the lipid groups of the stationary phase. More recently, our group has evidenced, for the first time, the ability of a 15-mer peptide with KLLL repeat, i.e., KLL(*KLLL*)$_2$KLLK, to translocate with low toxicity a nonspecific phosphorothioate oligodeoxynucleotide into glioma cells.[12] The capability of the above-mentioned 15-mer to form an amphipathic α-helix in aqueous solutions and organic solvents is now well established.[6,13] It is worth noticing that in numerous analyses, the hydrophobic core of membranes is modeled with organic solvents (methanol, ethanol, acetonitrile, and trifluorethanol), whereas their elementary structure is mimicked by lipid vesicles.[8] In fact, the above-mentioned 15-mer belongs to a family of peptides designed about 10 years ago and referenced in the literature as L_iK_j peptides ($i = 2j$).[5,6] The activity of these peptides against erythrocytes was again correlated to their ability to form α-helices.[5−7,14] Particularly, in a very detailed report based on Langmuir film balance, FT-IR, and polarization modulation IR spectroscopy (PMIRRAS),[6] the physicochemical properties of a series of seven peptides of this family (from 5- to 22-mer) at the air/water interface as well as their capacity to interact with dimyristoylphosphatidylcholine (DMPC) monolayers were discussed.[6] It was concluded that short peptides (more precisely the 5-mer and 9-mer) form intermolecular antiparallel β-sheets at the interface, whereas longer peptides (from 12- to 22-mer) form amphipathic α-helices. The analysis

* To whom correspondence should be addressed. E-mail: ghomi@smbh.univ-paris13.fr and ghomi@ccr.jussieu.fr. Tel.: +33-1-48388928 and +33-1-69874354. Fax: +33-1-48387356 and +33-1-69874360.

[†] Université Paris 13 and Université Pierre et Marie Curie.

[‡] Institut Pasteur.

[§] Present address: EA 3817, LNPC, UFR Biomédicale des Saints Pères, Université Paris Descartes, 45 rue des Saints-Pères, 75270 Paris cedex 06, France.

10.1021/jp074264k CCC: $37.00
Published on Web 10/06/2007

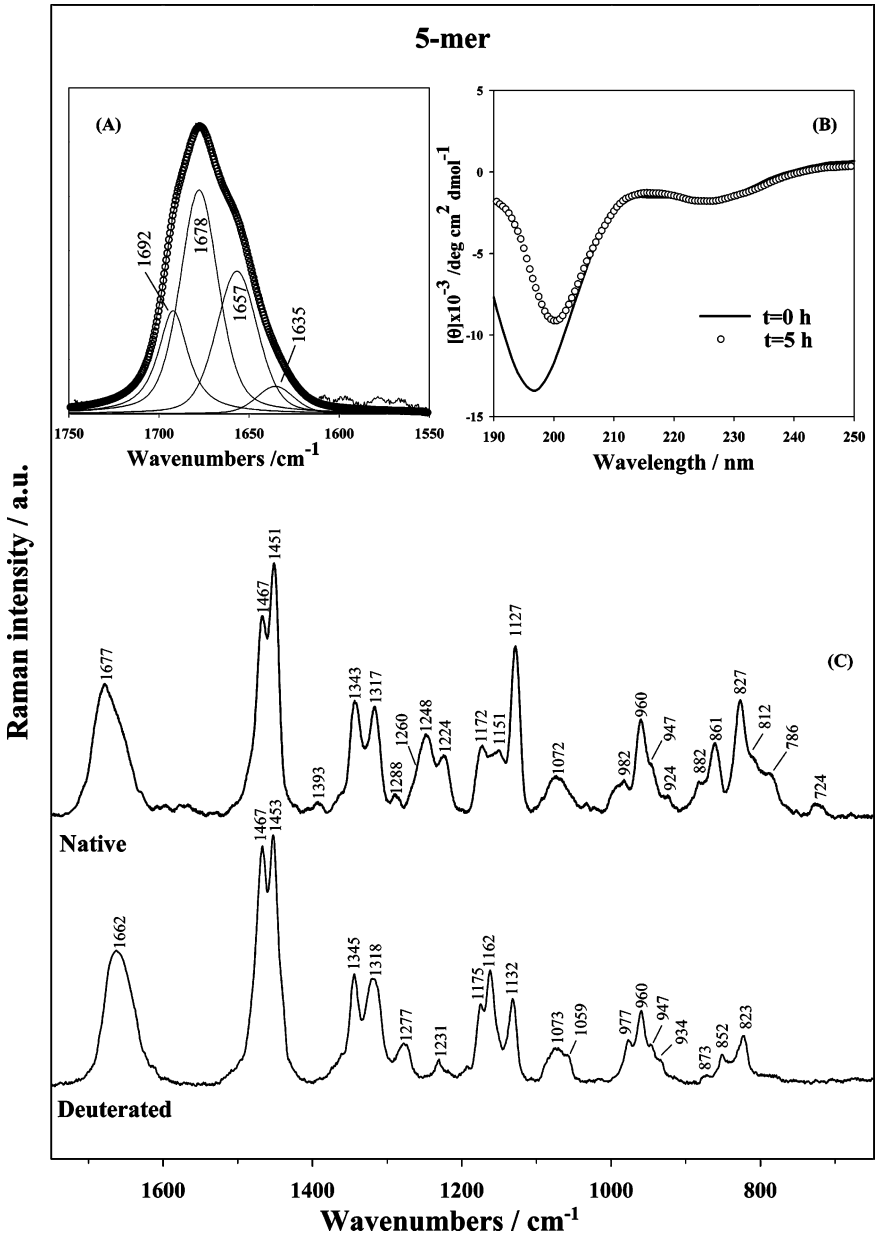

Figure 1. CD and Raman spectra of the 5-mer KLLLK recorded at room temperature in phosphate buffer. (A) Band decomposition in the amide I spectral region, 1750−1550 cm^{-1}; see Table 1 for assignments. (B) CD spectra recorded just after and 5 h after sample preparation (referred to as $t = 0$ and $t = 5$ h, respectively). (C) Comparison between the Raman spectra from native and labile hydrogen deuterated species of the peptide; 1750−650 cm^{-1} region is displayed.

of the amide I and amide II regions in the FTIR absorption spectra evidenced that all peptides are flat oriented at the air/water interface. On the other hand, it was postulated that the structure and orientation of the peptides were preserved upon interaction with the DMPC interface. However, all the mentioned FT-IR spectra[6] were observed from the methanol evaporation bulk samples, and Langmuir and PMIRRAS experiments were carried out at a very low concentration for peptides (sub-micromolar). It is also known that trifluoroacetate (TFA) contributes to an intense absorption band in the amide I region, rendering difficult the vibrational contribution of the peptide. To overcome these difficulties, we have combined two optical spectroscopic techniques, i.e., circular dichroism (CD) and Raman scattering, to characterize the LK-peptide conformational adaptability.[13] Following this approach, the behavior of a few LK peptides, especially those with $(KL)_n$ repeats, was evidenced in a concentration range from 100 μM to 5 mM as a function of chain length, molecular concentration, time, and environment (buffer, solvent). Particularly, we could emphasize the ability of Raman spectroscopy to analyze these systems when the use of CD spectroscopy alone can lead to eventual misinterpretation in secondary conformations. Indeed, in some cases, the superposition of CD signals arising from different conformers coexisting in solution can give rise to a complex "envelope signal" which renders difficult a suitable structural assignment. In this situation, the study of Raman spectra can considerably help to propose a reliable structural analysis. At last, the contribution of TFA anions to Raman spectra in amide I region is negligible.[13] In the present report, we apply this experimental protocol to the analysis of conformations and aggregation of the LK-peptides with $(KLLL)_n$ repeats.

II. Materials and Methods

Four cationic peptides, i.e., *KLLL*K, KLL*KLLL*KLLK, KLL*KLLLKLLL*KLLK, and KLL*KLLLKLLLKLLL*KLLK (KLLL

TABLE 1: Band Decomposition in the Amide I Region of the Raman Spectra for the Four Peptides Analyzed in This Work

peptides[a]	apparent maximum wavenumber[b]	decomposition[b]	area[c]	BWHH[d]	secondary structure assignments
5-mer	1677	1692	20	20	random
		1678	45	25	β-turn and loop
		1657	30	27	helix
		1635	5	25	β-sheet
11-mer	1667	1683	14	15	random
		1668	62	18	β-strand
		1652	18	14	helix
		1639	6	15	β-sheet
15-mer	1653	1653	100	23	helix
19-mer	1653	1653	100	20	helix

[a] 5-mer: KLLLK.11-mer: KLLKLLLKLLK.15-mer: KLLKLLLKLLLKLLK. 19-mer: KLLKLLLKLLLKLLLKLLK. [b] Wavenumbers are in cm^{-1}. [c] Area of each component is expressed in % (total area of the decomposed region is normalized at 100%). [d] BWHH: bandwidth at half-height (cm^{-1}).

repeat units shown in italics in each sequence) were synthesized at the Institut Pasteur (Paris) following a solid phase Fmoc procedure as previously described in detail.[12] For the sake of brevity these peptides are hereafter referred to as the 5-mer, 11-mer, 15-mer, and 19-mer, respectively. Purified peptides containing TFA as counterion were dissolved in phosphate buffer (containing 10 mM of K^+ and Na^+ cations, pH or pD 6.8) in PBS (phosphate buffer saline, containing an excess of 100 mM NaCl in solution, pH 7.4), in Tris (pH 7.4), in methanol, as well as in bicomponent mixtures containing the three latter buffers and methanol. For the 5-mer and 11-mer, the solubility in aqueous solution was enough in order to record CD and Raman spectra up to 5 mM. In the case of the 15-mer, a *foamy* solution is initially obtained. After a few minutes, the bubbles were gradually disappeared, enabling us to record Raman spectra with a reasonable scattering background. For the19-mer we could record both CD and Raman spectra at 2 mM because of the low water solubility of this peptide. However, it should be noticed that in both of the long chain peptides (15-mer and 19-mer), the solubility is considerably improved by adding methanol to the aqueous solution.

Dichroic signals from peptide samples as well as their variation as a function of temperature were analyzed on a JASCO J-810 spectrophotometer equipped with a Peltier accessory. Samples were placed in suprasil quartz cells (with path lengths of 0.01 mm or 1 mm). Each spectrum recorded in the 190−280 nm region corresponds to the average of five scans with a speed of 100 nm/min (5 min of accumulation). CD spectra of the buffer were used as the baseline in all experiments. The measured ellipticity for each sample, $[\theta]_{observed}$, was normalized to obtain the so-called mean residue ellipticity, $[\theta]$, by using the expression $[\theta] = [\theta]_{observed}/10ncl$, where n, c, and l are the number of residues in the peptide, the molar concentration, and the path length of sample, respectively.[15] Normalized ellipticity was expressed in deg cm^2 dmol^{-1}.

TABLE 2: Peak Positions and Tentative Assignments of the Raman Bands of the Four Peptides Recorded at Room Temperature in Phosphate Buffer[a]

5-mer		11-mer		15-mer		19-mer		tentative assignments
1677 (s)	*1662 (s)*							
		1667 (s)	*1656 (s)*		*1668 (sh)*		*1666 (sh)*	amide I
				1653 (s)	*1645 (s)*	1653 (s)	*1645 (s)*	
1467 (s)	*1467 (s)*	1466 (s)	*1467 (s)*	1464 (s)	*1464 (s)*	1465 (s)	*1465 (s)*	side chain, CH_3 and CH_2 bend
1451 (s)	*1453 (s)*	1451 (s)	*1452 (s)*	1449 (s)	*1451 (s)*	1451 (s)	*1451 (s)*	
1393 (w)	−	1396 (w)	−					
			1364 (sh)	1367 (w)	*1367 (w)*	1370 (w)	*1366 (w)*	side chain, CCH bend, C_α-bend
1343 (s)	*1345 (s)*	1343 (s)	*1345 (s)*	1345 (s)	*1346 (s)*	1346 (s)	*1346 (s)*	
1317 (s)	*1318 (s)*	1318 (s)	*1318 (s)*	1316 (s)	*1315 (s)*	1318 (s)	*1315 (s)*	
1288 (w)	−	1290 (w)	−	1293 (m)	−	1296 (m)	−	amide II
	1277 (m)		*1275 (m)*		*1271 (w)*		*1268 (w)*	
1260 (sh)	−	1260 (sh)	−	1262 (sh)	−	1262 (sh)	−	
1248 (m)	−	1245 (m)	−					
	1231 (w)		*1231 (m)*		*1235 (m)*		*1235 (m)*	backbone
1224 (m)		1220 (m)	−	1219 (m)	−	1221 (m)	−	
1172 (m)	*1175 (m)*	1172 (m)	*1174 (m)*	1172 (m)	*1174 (m)*	1174 (m)	*1173 (m)*	side chain, CH_3 rock
1151 (m)	*1162 (s)*	1150 (m)	*1162 (m)*	1152 (m)	*1142 (m)*	1154 (m)	*1142 (m)*	
1127 (s)	*1132 (m)*	1127 (s)	*1131 (m)*	1127 (s)	*1107 (w)*	1127 (s)	*1107 (w)*	
1072 (m)	*1073 (m)*					1077 (w)	−	
	1059 (sh)	1062 (m)	*1067 (w)*	1060 (w)	*1065 (w)*	1065 (sh)	*1058 (w)*	side chain, C−C str.
		1048 (sh)	−		*1028 (w)*		*1028 (w)*	
					1000 (w)			
982 (m)	*977 (m)*	981 (sh)	*981 (m)*	974 (sh)	−	972 (sh)	−	
960 (m)	*960 (m)*	960 (m)	*959 (m)*	958 (m)	*959 (s)*	959 (s)	*958 (s)*	side chain, CH_3 rock
947 (sh)	*947 (sh)*	948 (sh)		935 (m)	*930 (s)*	938 (s)	*930 (s)*	
924 (sh)	*934 (sh)*		*929 (m)*					
882 (sh)	*873 (w)*	883 (sh)	−	880 (sh)	*878 (sh)*	878 (sh)	*887 (w)*	
861 (m)	*852 (w)*	861 (m)	*855 (m)*	862 (m)	*856 (m)*	864 (m)	*856 (m)*	side chain, CH_2 wag, C−C str
			840 (m)					
827 (s)	*823 (m)*	830 (m)	*827 (m)*	827 (m)	*823 (m)*	830 (m)	*822 (m)*	
812 (sh)	−							
786 (sh)	−	794 (w)	−					
			752 (w)			770 (w)	−	
		738 (w)	*736 (sh)*	744 (w)	*742 (m)*	746 (m)	*741 (m)*	backbone, N-C-C bend
724 (w)	−					726 (sh)	*725 (w)*	

[a] 5-mer: KLLLK. 11-mer: KLLKLLLKLLK. 15-mer: KLLKLLLKLLLKLLK. 19-mer: KLLKLLLKLLLKLLLKLLK. Peak positions are in cm^{-1}. In italics are reported the wavenumbers observed upon labile hydrogen deuteration. In parentheses, s: intense, m: middle, w: weak, sh: shoulder.

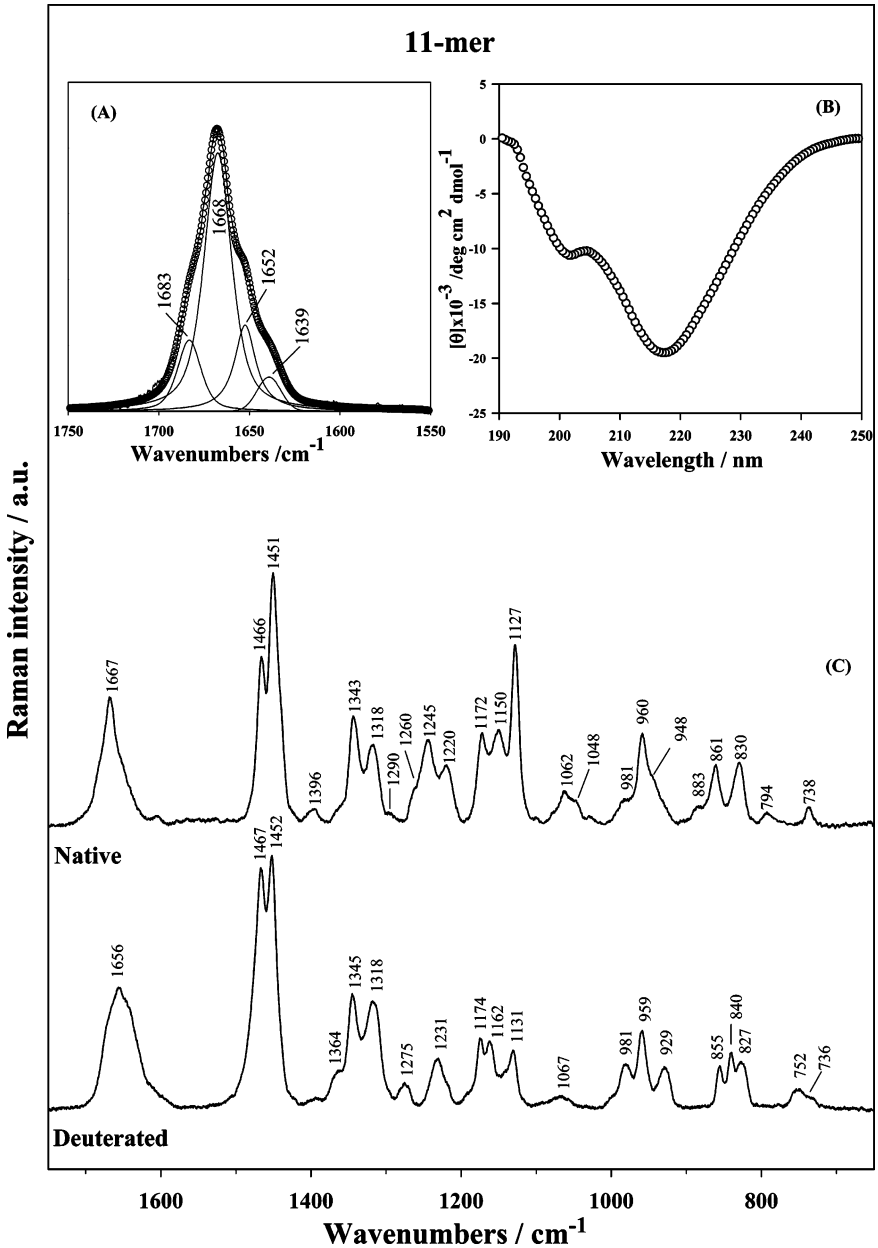

Figure 2. CD and Raman spectra of the 11-mer KLLKLLLKLLK recorded at room temperature in phosphate buffer. (A) Band decomposition in the amide I spectral region, 1750−1550 cm^{-1}; see Table 1 for assignments. (B) CD spectrum displayed in the 250−190 nm range. (C) Comparison between the Raman spectra from native and labile hydrogen deuterated species of the peptide; 1750−650 cm^{-1} region is displayed.

Samples used for recording Raman spectra were placed in a quartz suprasil microcell of 35 μL inner volume, excited with the 488 nm line of an Ar^+ laser (Stabilite model 2017-04S, Spectra Physics), and collected on a Jobin-Yvon T64000 spectrograph in a single spectrograph configuration with a 1200 grooves/mm holographic grating and a holographic notch filter. The spectrograph is equipped with a liquid nitrogen cooled CCD detection system (Spectrum One, Jobin-Yvon) based on a Tektronix CCD chip of 2000 × 800 pixels. The effective spectral slit width was set to ca. 5 cm^{-1}. Stokes Raman spectra were analyzed at room temperature in the 1750−650 cm^{-1} region (20 min of accumulation). The 19-mer spectra were also collected at 20 °C and 50 °C before and after a thermal annealing of the sample at 80 °C for 10 min. Buffer contribution was also recorded as a function of temperature and subtracted at each temperature from the Raman spectrum after normalization of both spectra to the water angular bending mode at 1645 cm^{-1}. TFA anion Raman bands were subtracted from the spectra recorded in peptide samples without any major difficulty as it was detailed in a preceding report of our group.[13] It should be pointed out that TFA provides a negligible contribution in the amide I and III regions taken as reference for secondary structural assignments. Analysis of the amide I region (1750−1550 cm^{-1}) of Raman spectra was performed by curve fitting as previously applied to vibrational spectra in order to probe the secondary conformations existing in the structure of peptides and proteins.[17−22] To decompose observed bands, mixed Gaussian + Lorentzian functions, with Lorentzian contribution kept equal to or greater than 50%, were employed. Initial guesses for their maximum wavenumbers were based on the second derivative analysis in the amide I region. Postprocessing of Raman spectra was performed using GRAMS/32 package (Galactic Industries). Figures shown in this paper were drawn using SIGMAPLOT (Systat Software Inc., Point Richmond, CA) package. Molecular models are drawn with GAUSSVIEW package (GAUSSIAN Inc.).

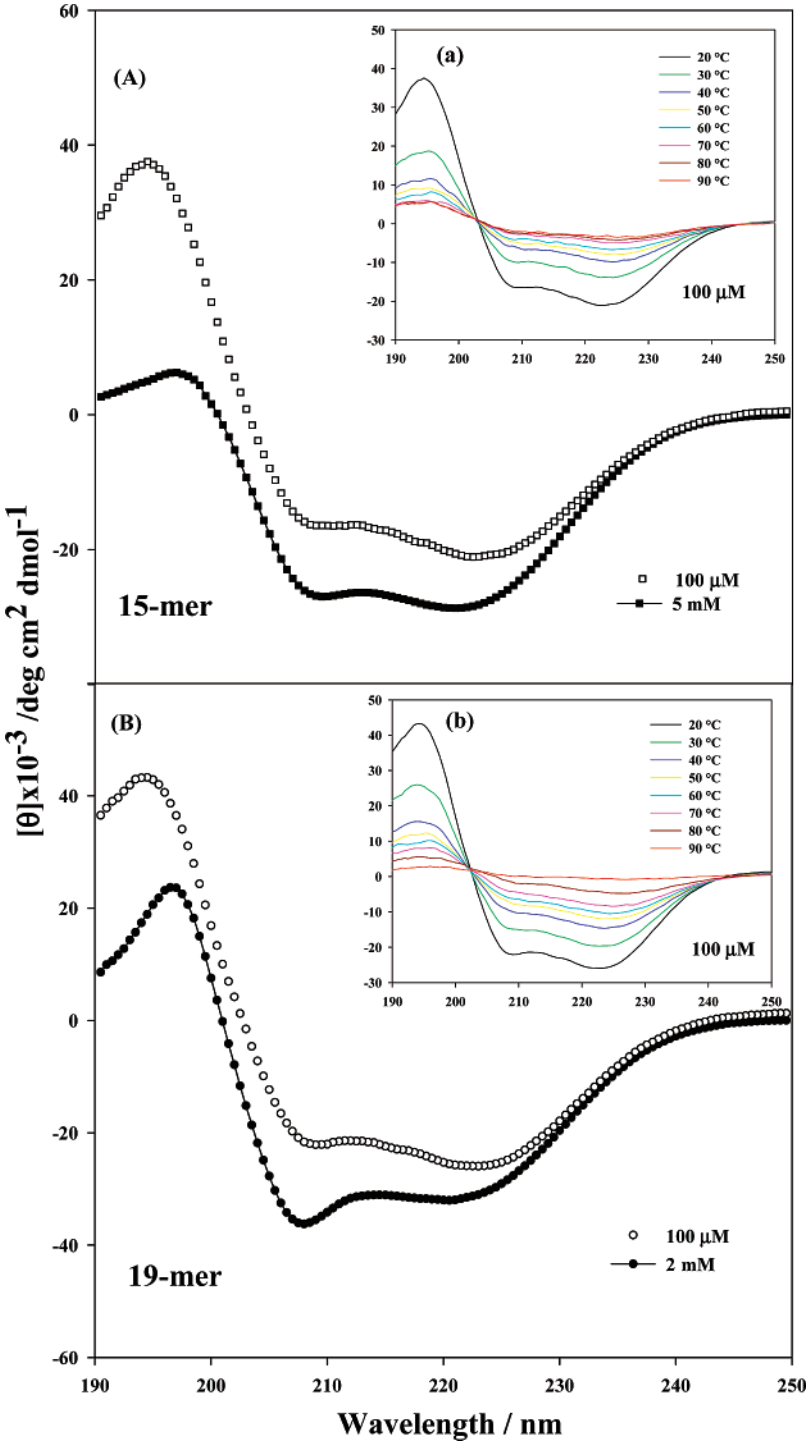

Figure 3. CD spectra of the 15-mer KLLKLLLKLLLKLLK and the 19-mer KLLKLLLKLLLKLLLKLLK recorded in phosphate buffer. (A) CD spectra of the 15-mer at 100 μM and 5 mM. (B) CD spectra of the 19-mer at 100 μM and 2 mM. CD spectra of the (a) 15-mer and the (b) 19-mer recorded at 100 μM as a function of temperature in the 20−90 °C range.

III. Results and Discussion

CD signal of the 5-mer (Figure 1B), revealing a disordered structure in a freshly prepared sample, characterized by a strong negative band at 198 nm,[23] undergoes a temporal evolution manifested by an intensity decrease accompanied with a redshift of the main minimum to ~200 nm (see spectrum obtained after 5 h). Raman spectrum of the 5-mer (Figure 1C) corresponds to a room temperature equilibrated sample analyzed several hours after sample preparation. Band decomposition in the amide I region (Figure 1A) allows us to assign about half of total conformers to β-type secondary structures (Table 1). However, a considerable population (~30%) of helical conformers may also exist in solution (Table 1). These results are in accordance with the observations in the amide III region of Raman spectra (Figure 1C), where a medium intensity band at 1248 cm^{-1} (β-type marker) and a weak component at 1288 cm^{-1} (helix marker), are observed (Table 2). A proportion of disordered conformers is also confirmed by a component at 1692 cm^{-1} (band decomposition in amide I region, Figure 1A, Table 1), and the corresponding amide III marker is observed as a shoulder at 1260 cm^{-1} (Figure 1C).

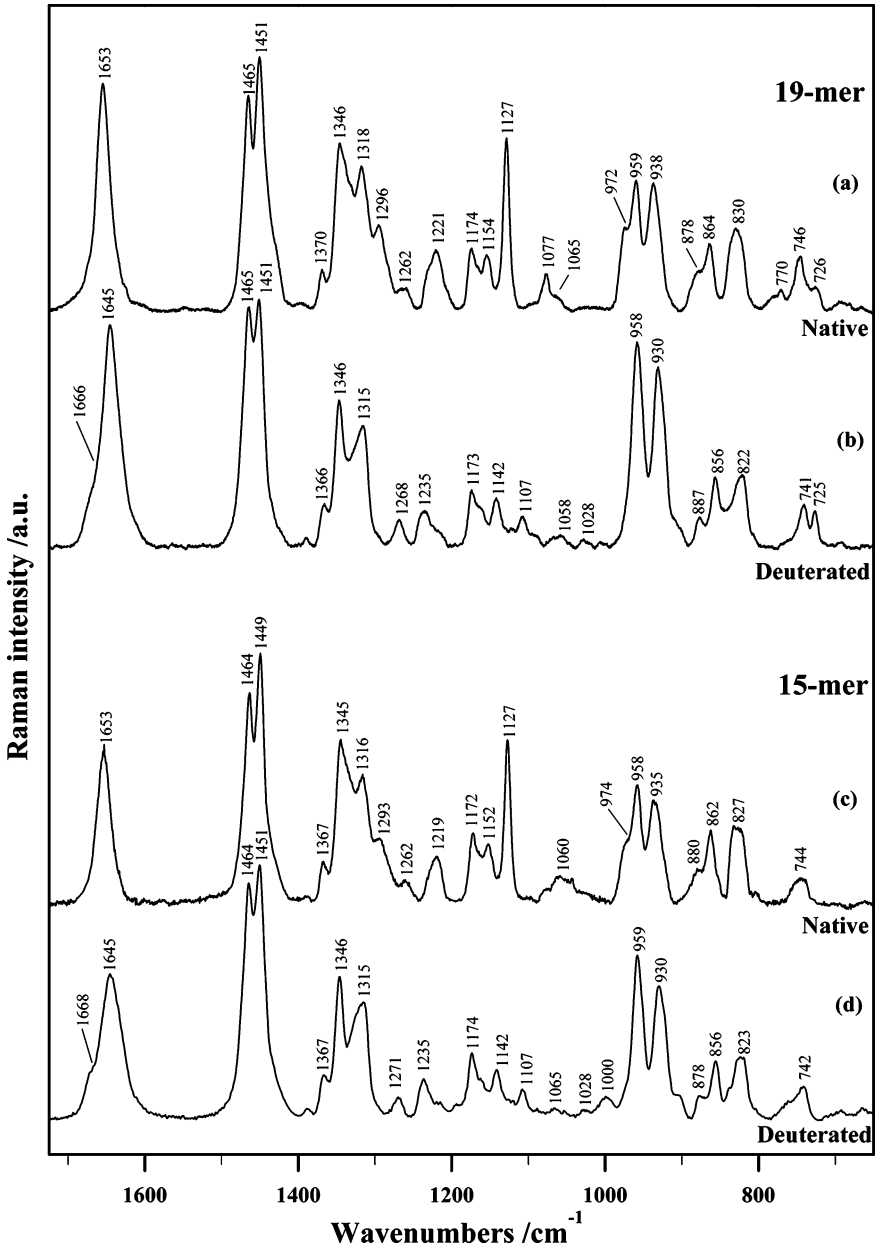

Figure 4. Comparison between the Raman spectra recorded at room temperature in phosphate buffer from the native and labile hydrogen deuterated species of the 19-mer, KLLKLLLKLLLKLLLKLLK (top), and the 15-mer, KLLKLLLKLLLKLLK (bottom), in the 1750−650 cm^{-1} region. Note that in the 19-mer the complete deuteration could be achieved by a thermal annealing at 80 °C during 10 min; see also Figure 5 and text.

The shape of the CD spectrum of the 11-mer undergoes a substantial change (Figure 2B) in comparison with that of the 5-mer (Figure 1B): an atypical signal (with no temporal evolution) characterized by two negative bands at ca. 200 and 218 nm was observed. The shape of the 11-mer CD spectrum leads us to suggest a possible coexistence of random and β-type structures in solution. The Raman spectrum shows a narrowing of the amide I region with a downshift of its apparent maximum to 1667 cm^{-1} (Figure 2C), being decomposed in Figure 2A and leading us to conclude an increase of β-type conformers of ~70%, Table 1). On the contrary, the helical and random populations are decreased in comparison with the 5-mer. In the amide III region, the β-marker appears as a resolved band at 1245 cm^{-1} (Figure 2C), and the helical marker is manifested by a very weak band observed at 1290 cm^{-1}.

Upon increasing chain length (caused by introducing additional KLLL repeats), i.e., in going from 11-mer to 15-mer and 19-mer, CD spectra change drastically (Figure 3A, B) and take a shape traditionally assigned to α-helical conformers in solution involving two negative bands at 208 and 222 nm with, however, a change in their relative intensity observed in the 19-mer as a function of concentration. In fact, at the lowest concentration (100 μM) where the level of aggregation is less important, both peptides show a 208 nm band less intense than that at 222 nm. The same spectral shape is found in the 15-mer even at a higher concentration (5 mM, Figure 3A), whereas in the 19-mer, an inversion of the intensity ratio is observed in going from 100 μM to 2 mM molecular concentration (Figure 3B). We will discuss again the effect of aggregation through the description of Raman spectra (deuteration and temperature-induced effects). The thermal stability of helical conformers in the 15-mer and 19-mer was analyzed by CD spectroscopy (peptides in phosphate buffer) at 100 μM and shown in insets a and b of Figure 3, respectively. In both cases, a general decrease of CD signal (about 400 times) with temperature is observed. The existence of an isobestic point in each case clearly

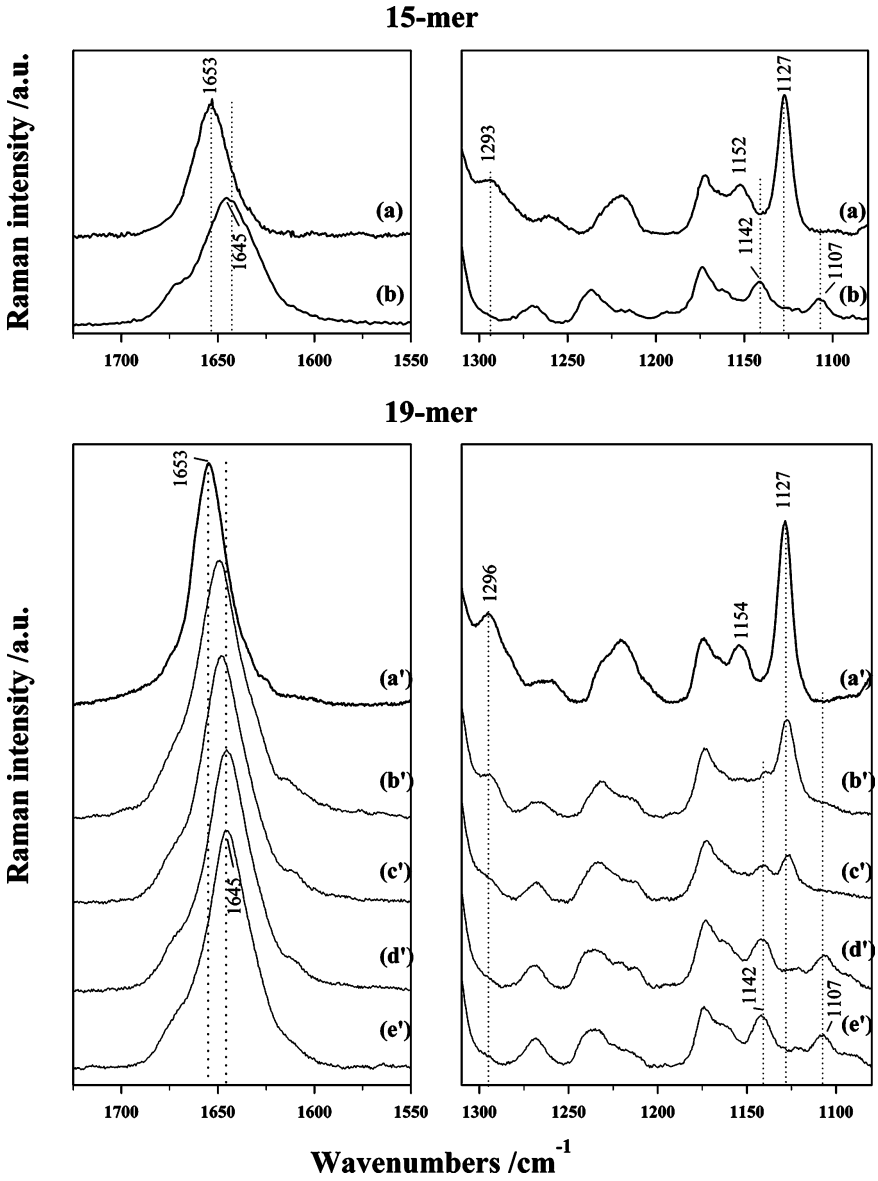

Figure 5. Effect of deuteration on the 15-mer KLLKLLLKLLLKLLK (top) and the 19-mer KLLKLLLKLLLKLLLKLLK in phosphate buffer. Two spectral ranges including first the amide I region (left) and second the amide III and 1127 cm^{-1} mode (right) are selected in order to emphasize the principal observed effects. (a, b) Raman spectra of the native and deuterated species of the 15-mer. Both spectra are obtained just after sample preparation at room temperature. Raman spectra of the 19-mer obtained (a′) in H_2O buffer at room temperature, (b′) in D_2O buffer at room temperature, (c′) in D_2O buffer at 50 °C, (d′) in D_2O buffer at 50 °C after a thermal annealing at 80 °C during 10 min, and (e′) in D_2O buffer at room temperature after the thermal annealing at 80 °C. In both peptides, Raman spectra were normalized to the intense bands in the 1460−1450 cm^{-1} region arising from CH_2 and CH_3 bending modes nonsensitive to deuteration.

shows a secondary structural transition. However a negative band at lower wavelengths assignable to disordered chains appears neither in the 15-mer nor in the 19-mer by increasing temperature. This may be interpreted by a possible compensation at low wavelength between the negative disordered chain CD signal and a positive one arising from helical conformers. Taken together, these results suggest that even at high temperature (90 °C), a population of helical conformers exists in solution. Further experiments on the basis of the analysis of Raman spectra as a function of temperature (not shown) proved again the high thermal stability of helical conformers. Room temperature Raman spectra of the 15-mer and 19-mer are displayed in parts c and a of Figure 4, respectively. The amide I region in both cases shows an intense single band at 1653 cm^{-1}, confirming the presence of only α-helical conformers in solution. Additional evidence for the helical secondary structure is the amide III marker observed at 1293 cm^{-1} and 1296 cm^{-1} for the 15-mer and the 19-mer, respectively.

The behavior of Raman spectra upon labile hydrogen deuteration should be emphasized. In the 15-mer, the amide I band maximum shows a 8 cm^{-1} downshift (Figure 5a,b), accompanied by the complete vanishing of the amide III marker at 1293 cm^{-1} in agreement with the complete deuteration of backbone labile hydrogens (NH) in this peptide. Assuming these criteria, the comparison of the Raman spectra of the 19-mer (Figure 5a′,b′) recorded at 20 °C in H_2O and D_2O, reveals an incomplete deuteration of this peptide. In order to access a complete isotopic substitution, we heated the peptide D_2O solution up to 80 °C during 10 min by recording at 50 °C the Raman spectra before and after this thermal annealing (Figure 5c′,d′). These spectra show that the heating process explained above allows us to perform a complete deuteration of the backbone labile hydrogens

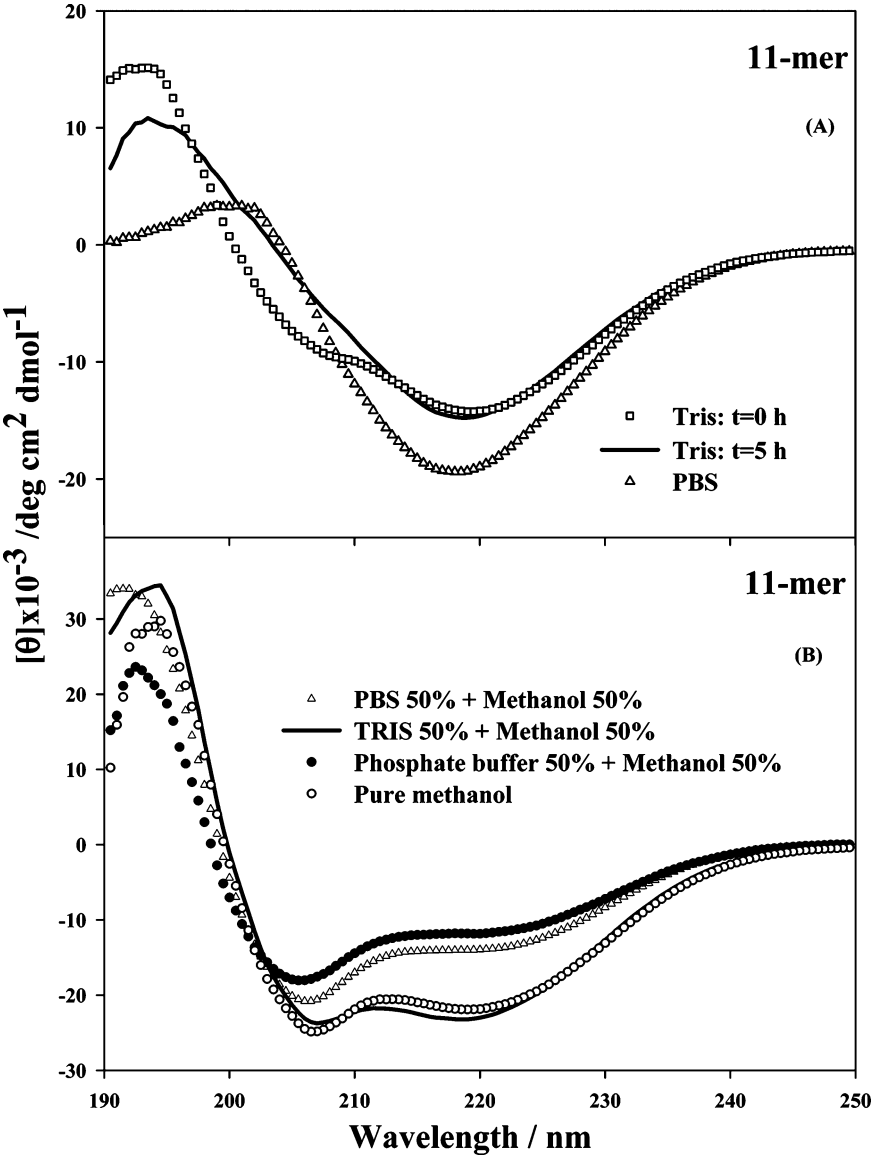

Figure 6. CD spectra of the 11-mer recorded in different environments. (A) CD spectra in PBS and Tris. Note that the CD spectrum recorded in Tris buffer shows a temporal evolution within a 5 h period: The initial spectrum ($t = 0$ h) is consistent with a mixture of conformations, and the final one ($t = 5$ h) reveals the presence of β-type secondary structures in solution. (B) CD spectra recorded in methanol and in bicomponent aqueous buffers containing methanol. All spectra reveal the presence of helical type conformers in solution.

in the 19-mer. Finally, the Raman spectrum recorded at 20 °C after annealing (Figure 5e′) shows the same features in the amide I and III regions as observed and explained above in the 15-mer (Figure 5b). The Raman spectrum of the 19-mer recorded at room temperature after the above-mentioned thermal annealing is displayed in Figure 4b for comparison.

Another prominent effect that merits to be noticed is the behavior of the intense Raman mode observed at 1127 cm^{-1} upon deuteration. In the two shorter peptides (5-mer and 11-mer), the intensity of this mode decreases in deuterated species, and its maximum suffers an *upshift* to ca. 1132 cm^{-1} (Figures 1 and 2), whereas in the longer peptides (15-mer and 19-mer) a *downshift* to 1107 cm^{-1} appears (Figures 5a,b and 5a′−e′). In addition, a more important intensity decrease upon deuteration is observed in the longer peptides compared to that in the shortest ones.

In order to elucidate the origin of the 1127 cm^{-1} mode, we have recorded a series of Raman spectra in aqueous solutions of amino acids and short peptides (i.e., L,[24] K, KL, KLK, and LKL; spectra not shown). The overall examination of all these data led us to confirm that the 1127 cm^{-1} mode observed in the four presently reported peptides originates from leucine resuidue. As reported previously, vibrational spectra of leucine present an intense mode at 1134 cm^{-1} showing a downshift to 1129 cm^{-1} in D_2O solution.[24] Quantum mechanical calculations permitted the assignment of this mode principally to the CCH bending and C−C stretch motions of the leucine side chain. Raman spectrum of a leucine-containing peptide reveals a (more or less) intense mode at 1127 cm^{-1}. This effect is observed whatever the peptide chain length is. It means that the 1127 cm^{-1} mode appears when at least a peptide bond is formed with a leucine residue. Upon all our observations, we can thus explain the behavior of this mode upon deuteration as follows: (i) in the 5-mer and 11-mer, both containing a random population (Table 1), a similar isotopic effect is observed: 1127 → 1132 cm^{-1} (as measured in a completely random chain like the 3-mer KLK, data not shown); (ii) conversely, in the 15-mer and 19-mer, where the majority of conformers adopt a helical structure, the behavior of this mode is definitely different: 1127 → 1107 cm^{-1}. We interpret this difference as arising from a stronger coupling of the 1127 cm^{-1} band to the peptide backbone in helical chains, presumably due to the formation of intramolecular

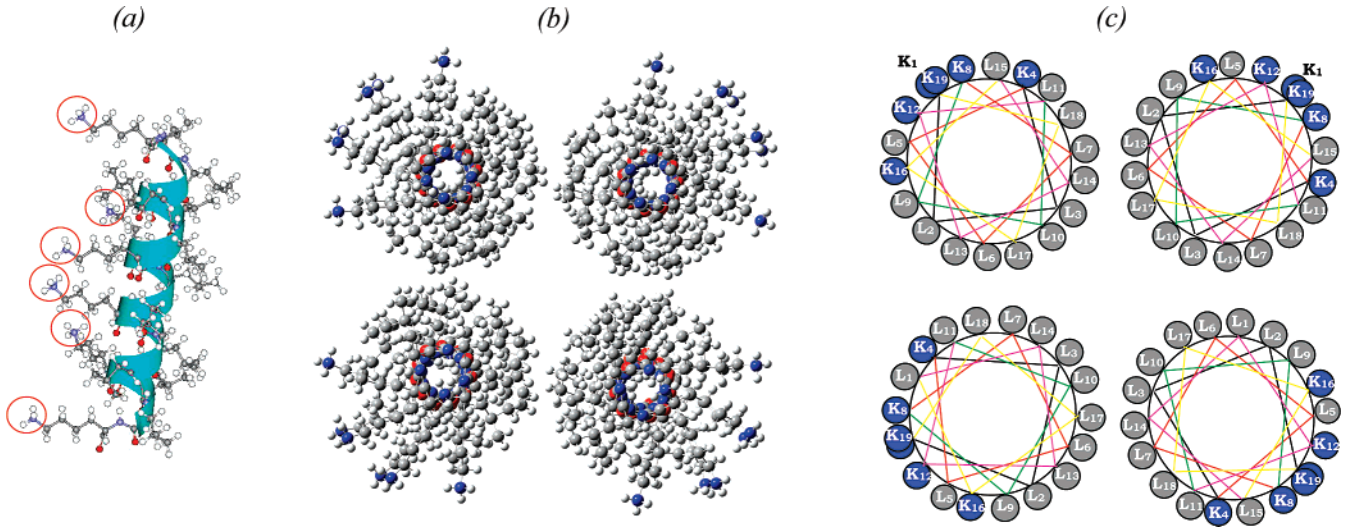

Figure 7. Graphic presentation of the 19-mer KLLKLLLKLLLKLLLKLLK and its probable aggregates. (a) The 19-mer in an ideal α-helical form, viewed perpendicularly to the helix axis. The backbone chain is in a ribbon form, and the charged heads (NH_3^+) of lysines are surrounded by red circles, to emphasize the amphipathic character of the helix. (b) An ideal symmetrical bundle formed by four α-helices, seen parallel to the helix axis (nitrogen in blue, oxygen in red, carbon in gray, and hydrogen in white). (c) Same bundle using a wheel presentation for peptide residues. Note the hydrophobic channel formed in the inner part of a four-membered bundle by leucine residue side chains.

H-bonds between C═O and N−H groups along the backbone. Another effect which confirms this assumption can be seen in Figure 5, where both the 1127 cm^{-1} and 1296 cm^{-1} (helix amide III marker, signature of a −C═O···H−N− hydrogen bond in a helical backbone) vanish simultaneously upon deuteration, either in the 15-mer (Figure 5a,b) or in the 19-mer (Figure 5a′−e′).

IV. Concluding Remarks

This report provides several examples of evidence concerning the role of the building block as well as the environmental dependence of the secondary structure of the LK peptides with KLL(KLLL)$_n$KLLK primary sequence. An overall examination of the presently described results as well as those previously reported by Castano et al.[6] allows us to present a global description of the conformational behavior of these peptides:

Previously published results[6] had suggested an antiparallel β-sheet conformation for the peptides containing less than 12 amino acids and a helical structure for those with longer chains. The two shorter peptides analyzed in the present work, i.e., the 5-mer and the 11-mer, present a mixture of secondary structures in phosphate buffer (disordered, β-type, and helical chains). The existence of several populations in a very short peptide such as the 5-mer, does not really seem to be surprising. But, the increase of the β-strand population in the 11-mer observed in phosphate buffer led us to perform additional experiments in order to confirm whether the conformational equilibrium in solution is environment dependent. We show here two series of CD experiments: (i) those observed in PBS and Tris buffers (Figure 6A) where an excess of salt exists in solution compared to that in phosphate buffer, see Materials and Methods, and (ii) those in methanol as well as its bicomponent mixtures with phosphate buffer, PBS, and Tris (Figure 6B). The first series of experiments (in PBS and Tris buffers) proves the stabilization of β-type conformers, as manifested by a negative band at ca. 220 nm. However, a slower conformational evolution is observed in Tris, where a few hours were necessary in order to obtain a CD spectrum characteristic of the β-type secondary structure (Figure 6A). In contrast, the presence of methanol leads to the stabilization of helical conformers. The conformational equilibrium shift observed in the 11-mer upon environmental change reveals again the influence of methanol as a solvent with a low dielectric constant, favoring the stabilization of intramolecular interactions and consequently helical conformers.[13,24] These solute−solvent interactions compensate, in evidence, the shortness of the 11-mer to adopt a stable helical conformation in phosphate buffer (only two complete α-helical turns are expected in this peptide). An excess of salt and especially that of Cl^- anions might be responsible for a positive charge screening of lysine residues, presumably via interactions with water molecules, favoring a preferential formation of β-strands. The gradual stabilization of β-type conformers in Tris buffer with time should be in fact due to the capability of a Tris molecule to establish H-bond interactions with a peptide chain, thus retarding the accomplishment of β-strand formation. The 15-mer and 19-mer, both capable of forming at least three and four complete helical turns, respectively, have obviously the necessary length to induce and stabilize stable helical conformers as the major population in solution.

The other interesting effect mentioned here is the analysis of aggregate formation in the 15-mer and 19-mer solutions. This was offered to us through the labile hydrogen deuteration experiments in both peptides. In fact, as mentioned earlier,[25−29] helix−helix interactions can be stabilized by means of hydrophobic interactions. In amphipathic helices, such as those under study in this report, leucine-rich helical faces can establish this kind of interaction. A model of a possible helix bundle (with four interacting helices) is displayed in Figure 7. We have mentioned above the relatively low solubility of the 15-mer and 19-mer in aqueous solution, especially at millimolar concentrations. The obtention of a homogeneous solution after a few minutes can be somehow explained by this kind of aggregation. This model also makes a hydrophobic channel formed inside the bundle appear, rendering difficult a possible exchange between the peptide backbone and water (or heavy water) molecules. This lack of water accessibility increases with the helix length, thus explaining the deuteration retard of backbone N−H groups in the 19-mer. The thermal annealing necessary to accomplish a complete deuteration in the 19-mer is in fact an indirect manner to decrease helix−helix hydrophobic interactions by increasing the thermal mobility of bundle components, so rendering possible the penetration of heavy water in the vicinity of helices. Previously, a model with flat oriented helices

at the air/water interface was proposed for both the 15-mer and 19-mer on the basis of PMIRRAS experiments performed at low peptide concentrations.[6] This model cannot interpret the deuteration effects observed in the 19-mer in much higher concentrations (at least 20 times higher). Thus, it is possible to imagine that at low concentration, noninteracting amphipathic peptide chains present a flat orientation at the air/water interface. Upon increasing concentration, helix bundles may be formed with an external hydrophilic face, leading gradually to the complete immersion of aggregated peptide chains.

Generally, peptide aggregation plays a pivotal role in control drug release,[30] especially in the framework of in vitro DNA or gene transfer strategies by the use of cationic peptides as vectors.[31] Antimicrobial and hemolytic effects of a series of minimalist cationic 12-mer peptides with the generic primary sequence N^{ter}-KXXXKWXXKXXK (where X = G, A, V, I, or L) were reported previously.[32] Especially, correlation was made with both the secondary structure and the aggregation capacity of these peptides. It was emphasized (Fourier transform infrared absorption data) that the leucine-containing peptide (X = L) whose sequence composition presents some similarity with that of the 11-mer studied in this report, except its size is between the 11-mer and the 15-mer, it exists in aggregate state (fluorescence data on rhodamine labeled peptide), and it presents a major population of helical secondary structure when incorporated in the PE/PG multi-bilayers. This peptide also presents a considerable antimicrobial (and hemolytic) level. Similar experiments are now necessary in order to analyze the mode of interaction of the α-helix forming peptides presented here with model membranes as a function of their peptide chain length, secondary structure, hydrophobic/lipophilic balance, and concentration. This will help us to better understand our encouraging results obtained on the vectorization of oligonucleotides into glioma cells by means of the 15-mer LK-peptide.[12]

References and Notes

(1) DeGrado, W. F.; Lear, J. D. *J. Am. Chem. Soc.* **1985**, *107*, 7684−7689.

(2) Cornut, I.; Thiaudière, E.; Dufourcq, J. In *The Amphipathic Helix*; Epand, R. M., Ed.; CRC Press: Boca Raton, FL, 1993; pp 173−219.

(3) Saberwal, G.; Nagaraj, R. *Biochim. Biophys. Acta* **1994**, *1197*, 109−131.

(4) Maloy, W. L.; Kari, U. P. *Biopolymers* **1995**, *37*, 105−122.

(5) Castano, S.; Cornut, I.; Büttner, K.; Dasseux, J. L.; Dufourcq, J. *Biochim. Biophys. Acta* **1999**, *1416*, 161−175.

(6) Castano, S.; Desbat, B.; Laguerre, M.; Dufourcq, J. *Biochim. Biophys. Acta* **1999**, *1416*, 176−194.

(7) Blondelle, S.; Houghten, R. A. *Biochemistry* **1992**, *31*, 12688−12694.

(8) Blondelle, S. E.; Lohner, K.; Aguilar, M. I. *Biochim. Biophys. Acta* **1999**, *1462*, 89−108.

(9) Maget-Dana, R.; Lelievre, D. *Biopolymers* **2001**, *59*, 1−10.

(10) Niidome, T.; Takaji, K.; Urakawa, M.; Ohmori, N.; Wada, A.; Hirayama, T.; Aoyagi, H. *Bioconjug. Chem.* **1999**, *10*, 773−780.

(11) Dufourcq, J.; Neri, W.; Henry-Toulmé, N. *FEBS Lett.* **1998**, *421*, 7−11.

(12) Boukhalfa-Heniche, F. Z.; Hernandez, B.; Gaillard, S.; Coïc, Y. M.; Huynh-Dinh, T.; Lecouvey, M.; Seksek, O.; Ghomi, M. *Biopolymers* **2004**, *73*, 727−734.

(13) Hernandez, B.; Boukhalfa-Heniche, F. Z.; Seksek, O.; Coïc, Y. M.; Ghomi, M. *Biopolymers* **2006**, *81*, 8−19.

(14) Cornut, I.; Buttner, K.; Dasseux, J. L.; Dufourcq, J. *FEBS Lett.* **1994**, *349*, 29−33.

(15) Lazo, N. D.; Downing, D. T. *J. Peptide Res.* **2001**, *58*, 457−463.

(16) Silva, R. A. G. D.; Yasui, S. C.; Kubelka, J.; Formaggio, F.; Crisma, M.; Toniolo, C.; Keiderling, T. A. *Biopolymers* **2002**, *65*, 229−243.

(17) Maiti, N. C.; Apetri, M. M.; Zagorski, M. G.; Carey, P. R.; Anderson, V. E. *J. Am. Chem. Soc.* **2004**, *126*, 2399−2408.

(18) Munishkina, L. A.; Phelan, C.; Uversky, V. N.; Fink, A. L. *Biochemistry* **2003**, *42*, 2720−2730.

(19) Debelle, L.; Alix, A. J. P.; Wei, S. M.; Jacob, M. P.; Huvenne, J. P.; Berjot, M.; Legrand, P. *Eur. J. Biochem.* **1998**, *258*, 533−539.

(20) Barth, A.; Zscherp, C. *Quart. Rev. Biophys.* **2002**, *35*, 369−430.

(21) Surewicz, W. K.; Mantsch, H. H.; Chapman, D. *Biochemistry* **1993**, *32*, 389−394.

(22) Dong, A.; Kendrick, B.; Kreilgard, L.; Matsuura, J.; Manning, M. C.; Carpenter, J. F. *Arch. Biochem. Biophys.* **1997**, *347*, 213−220.

(23) Chou, P. Y.; Fasman, G. D. *Biochemistry* **1974**, *13*, 211−222.

(24) Derbel, N.; Hernandez, B.; Pflüger, F.; Liquier, J.; Geinguenaud, F.; Jaïdane, N.; Ben-Lakhdar, Z.; Ghomi, M. *J. Phys. Chem. B* **2007**, *111*, 1470−1477.

(25) Cammers-Goodwin, A.; Allen, T. J.; Oslik, S. L.; McClure, K. F.; Lee, J. H.; Kemp, D. S. *J. Am. Chem. Soc.* **1996**, *118*, 3082−3090.

(26) Gilson, M. K.; Honing, B. *Proc. Natl. Acad. Sci.* **1989**, *86*, 1524−1528.

(27) Jaikaran, D. C. J.; Biggin, P. C.; Wenschuh, H.; Sansom, M. S. P.; Woolley, G. A. *Biochemistry* **1997**, *36*, 13873−13881.

(28) Gibney, B. R.; Rabanal, F.; Reddy, K. S.; Dutton, P. L. *Biochemistry* **1998**, *37*, 4635−4643.

(29) Johansson, J. S.; Scharf, D.; Davies, L. A.; Reddy, K. S.; Eckenhoff, R. G. *Biophys. J.* **2000**, *78*, 982−993.

(30) Sal-Man, N.; Gerber, D.; Shai, Y. *J. Biol. Chem.* **2005**, *280*, 27449−27457.

(31) Dalluge, R.; Haberland, A.; Zaitsev, S.; Schneider, M.; Zastrow, H.; Sukhorukov, G.; Böttger, M. *Biochim. Biophys. Acta* **2002**, *1576*, 45−52.

(32) Avrahami, D.; Oren, Z.; Shai, Y. *Biochemistry* **2001**, *40*, 12591−12603.